Eidgenössische Technische Hochschule Zürich
Swiss Federal Institute of Technology Zurich

Autonomous Systems Lab
Prof. Roland Siegwart

Semester Thesis

Sensing and characterization of the motor dynamics on an omnidirectional flying vehicle

Spring Term 2020

Supervised by:
Weixuan Zhang
Maximilian Brunner

Author:
Fausto Tapia

ETH

Eidgenössische Technische Hochschule Zürich
Swiss Federal Institute of Technology Zurich

Declaration of originality

The signed declaration of originality is a component of every semester paper, Bachelor's thesis, Master's thesis and any other degree paper undertaken during the course of studies, including the respective electronic versions.

Lecturers may also require a declaration of originality for other written papers compiled for their courses.

I hereby confirm that I am the sole author of the written work here enclosed and that I have compiled it in my own words. Parts excepted are corrections of form and content by the supervisor.

Title of work (in block letters):

Sensing and characterization of the motor dynamics on an omnidirectional flying vehicle

Authored by (in block letters):

For papers written by groups the names of all authors are required.

Name(s):	**First name(s):**
Tapia Benavides	Fausto

With my signature I confirm that

- I have committed none of the forms of plagiarism described in the 'Citation etiquette' information sheet.
- I have documented all methods, data and processes truthfully.
- I have not manipulated any data.
- I have mentioned all persons who were significant facilitators of the work.

I am aware that the work may be screened electronically for plagiarism.

Place, date	**Signature(s)**
20.07.2020	

For papers written by groups the names of all authors are required. Their signatures collectively guarantee the entire content of the written paper.

Contents

Preface

Bla bla ...

Abstract

Hier kommt der Abstact hin ...

Symbols

Symbols

τ	Throttle command
V	Voltage
ω	Angular Speed

Indices

x	x axis
y	y axis

Acronyms and Abbreviations

ETH	Eidgenössische Technische Hochschule
ASL	Autonomous Systems Lab
BLDC	Brush-less Direct Current
PMSM	Permanent Magnet Synchronous Motor
ESC	Electronic Speed Controller
FC	Flight Controller
MAV	Micro Aerial Vehicle
OMAV	Omni-directional Micro Aerial Vehicle
DOF	Degree of Freedom
PWM	Pulse Width Modulation
FOC	Field Oriented Control
EMF	Electro Motive Force
UART	Universal Asynchronous Receiver/Transmitter protocol
UAVCAN	Uncomplicated Application-level Vehicular Communication And Networking
CAN	Controller Area Network

Chapter 1

Introduction

In the past decade, multi-copter type drones have been developed and spread all around the world for applications ranging from geographical mapping to entertainment. Furthermore, the latest developments on Miniature Aerial Vehicles (MAVs) have involved more physical interactions with the environment, power optimization and more Degrees of Freedom (DoFs) which leads to significantly more complex control pipelines. For instance, the Omnidirectional Miniature Aerial Vehicle (OMAV) at the Autonomous Systems Lab (ASL) in ETH Zurich and outlined in [1] consists of 6 pairs of co-axially aligned propellers with tilting axis. Mentioned platform is depicted in Figure 1.1.
Although this novel setup is highly versatile, the current rotor speed control implementation is open-loop, assuming relatively accurate and linear throttle to actual rotor speed mapping. Furthermore, the high number of propellers increases the chance of an individual failure on flight, requiring status information to be sent towards the flight controller (FC). Another important consideration is the aerodynamic interference between coaxial propellers, which surely causes disturbances leading to slower tracking. The extend of this disturbances is still unknown. Therefore, [2] recommends to perform a more thorough identification of this OMAV dynamics to decrease disturbances during optimal control design.
Objectives In this context, this report will describe my work during my semester project with the following objectives:

- Familiarize with current firmware available for FC-ESC communication.
- Achieve rotor speed feedback from the ESC to the FC.

Figure 1.1: ASL OMAV

- Explore different ESC typologies and
- Investigate the characteristics of driving the Brush-less Direct Current (BLDC) motors using an ESC.
- Investigate features available in modern ESCs.

Chapter 2

Literature Review

2.1 Brush-less DC motor driving

2.1.1 Brush-less DC motor

Most UAV platforms spin their propellers using Brushless-DC (BLDC) motors due to their low weight, high top speeds and efficiency. Therefore, it is imperative to know the basic principles to analyze ESCs.
A BLDC motor can be 1, 2 or 3-phase. However, the most efficient version at high speeds and the ones used for UAVs is the 3-phase version. Therefore, the BLDC term will refer to 3-phase BLDC motors. Figure 2.1 shows a simplified diagram with only 4 magnetic poles whereas a typical motor used for UAVs would have 14. Here,the stator includes coils and the rotor has permanent magnets.

2.1.2 BLDC motor driving methods

Two configurations can be used to run BLDC motors as mentioned in [4], both based on Pulse Width Modulation (PWM). These are Trapezoidal and Sinusoidal. They differ in the ideal driving voltage wave-forms to use when driving the motor coils. In both cases, the best performing phase shift between phases is 120°. The effective instantaneous voltage in each coil is a fraction of the DC power supply. PWM approximates this fraction by providing a pulsing signal with a corresponding duty cycle (fraction of time the signal is high). To generate these PWM signals from a DC power source, power MOSFETs are used in bridge configurations. The

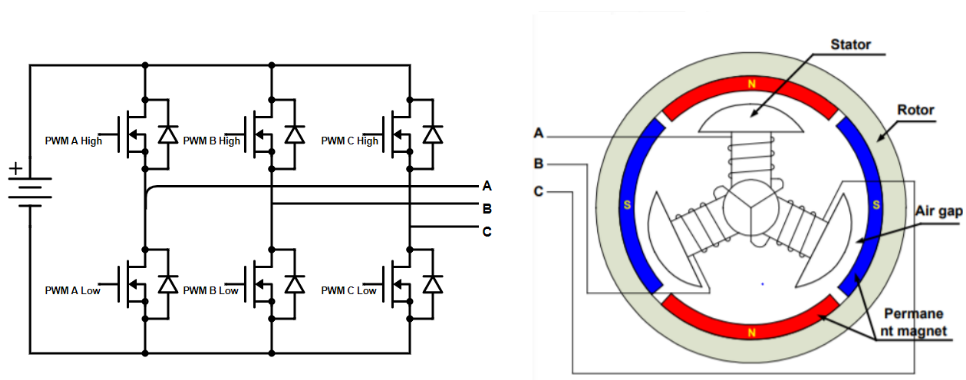

Figure 2.1: *Left* MOSFET bridge driver. *Right* BLDC motor simplified [3]

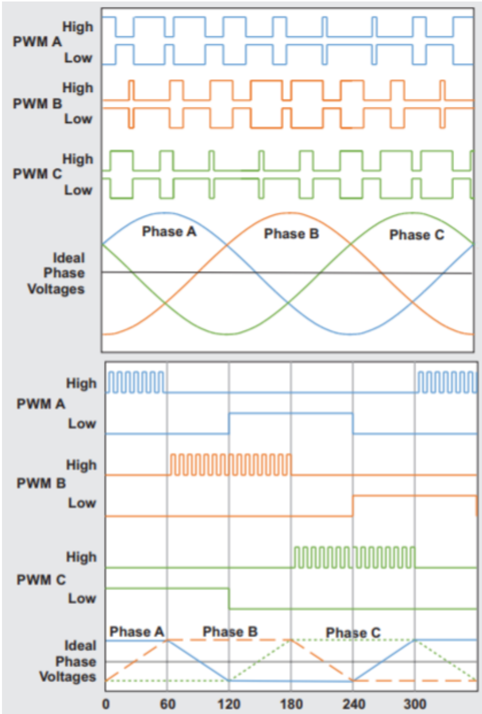

Figure 2.2: PWM Phase signals vs Rotor Position. *Top* Sinusoidal FOC, *Bottom* Trapezoidal. Adapted from [4]

specific configuration used for BLDC motors is shown in Figure 2.1

Trapezoidal: Here the ideal driving waveform is a trapezoidal wave. As shown in Figure 2.2 bottom. This method is easier to implement in hardware since a relatively low accuracy in rotor angular position estimation is needed. However, there are significant power loses caused by many spikes in the signal and also because the electrical magnetic field caused by the stator is only instantaneously at the optimal orientation relative to the rotor magnetic field (perpendicular). Here, the duty cycle put through the active phases is constant for the same rotor speed

Sinusoidal: In this case, the ideal driving waveform is a sinusoid as seen in figure 2.2 top. Note that for the same rotor speed, the duty cycle continuously changes over an electrical period to mimic the ideal sinewave. This is because of the waveform continuously changing and because feedback control [1] is used to maintain the relative orientation rotor-startor magnetic field orientation optimal (90°). Since the duty cycle is changed more often and depending on the rotor position, this method requires a significantly higher accuracy in rotor angular position estimation. Higher efficiency is obtained in two fronts:less pulsing implies less spikes and therefore switching power losses; the magnetic fields relative orientation is controlled to be optimal.

[1] This is not rotor speed control

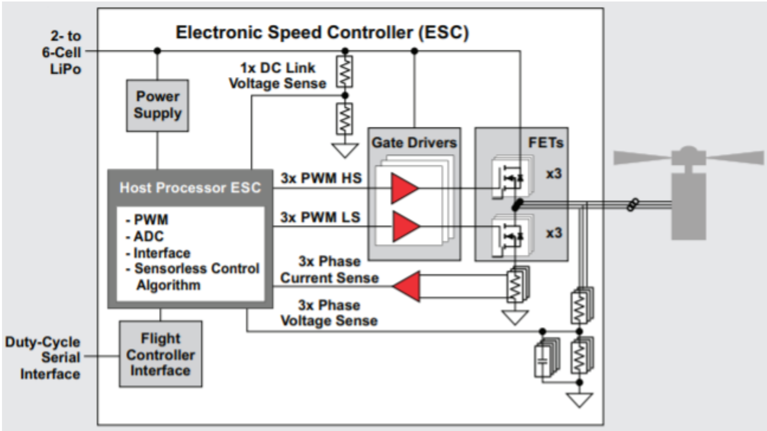

Figure 2.3: ESC general architecture [4]

2.2 Electronic Speed Controllers

2.2.1 General structure

The circuits that run the BLDC motors are commonly known as Electronic Speed Controllers (ESC). However, the majority of current available ones do not perform direct motor speed control. Their core components are a micro-controller, gate drivers, back Electro-motive foce (EMF) measurement resistors and the MOSFETs (shown in Figure 2.1). In essence, what they do is receive a throttle signal from a Flight Controller (FC) representing the amplitude of the ideal driving signal (explained in previous subsection, Fig. 2.2). The diagram in Figure 2.3 shows a general electrical architecture of ESCs. Note that gate drivers are simply interface circuits that allow to turn on/off the MOSFETs.

2.2.2 Communications

ESCs need to communicate with the FC to receive throttle commands and in some cases they also send status messages. Hence, some protocols have been used and other have been developed in the context of UAVs.

Analog Protocols

All of these protocols are based on Pulse width modulation given a maximum and a minimum pulse width to be set as maximum and minimum throttle. Hence, these protocols are commonly called RCPWM. Thee different protocols in this category merely differ in the pulse period. Figure 2.4 depicts these kind of signals on the top and Table 2.1 shows their transmission parameters.

Digital Protocols

Even though most of these protocols are widely known as digital, the true purely digital protocol is UAVCAN. The rest define certain specific pulse time durations to high or low. Dshot will be explained thoroughly in particular given that it's the basis of all the other methods but UAVCAN.
Dshot: This method consists of a 16-bit packet streamed continuously. Each bit is encoded as a pulse with one of to widths, depending on the pulse width version. Figure 2.5 shows the typical DShot signal and the information organization in each packet. The packet is divided into three sections:

Figure 2.4: Oneshot protocol [5]

Table 2.1: ESC protocols' speeds

Protocol	Type	Pulse width range [μs]	Max Update Rate [kHz]
PWM	Analog	1000 - 2000	2000
Oneshot125	Analog	125 - 250	250
Oneshot42	Analog	42 - 84	84
Multishot	Analog	5 - 25	40
Dshot150	Digital	2.5, 5*	9
Dshot300	Digital	1.25, 2.5*	18
Dshot600	Digital	0.625, 1.25*	37
Dshot1200	Digital	0.312, 0.625*	75
Bidirectional Dshot	Digital	Same as Dshot	Same as Dshot
Proshot	Digital	Same as Dshot	Same as Dshot
UAVCAN	Digital	NA	NA

* Pulses can only take either of the two values (Digital)

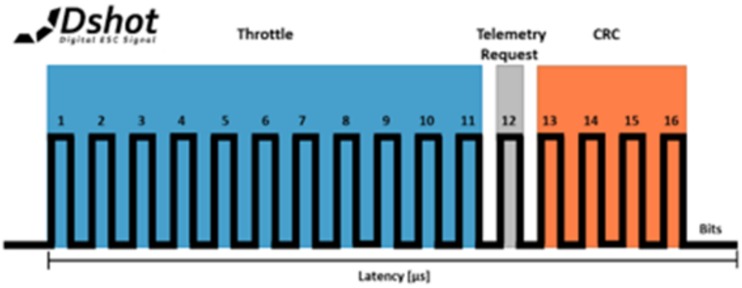

Figure 2.5: Dshot Signal Structure [6]

- Throttle command: Consists of 11 bits (Decimal values 0 -2047). Commands in the range [0,47] are status request commands whereas values in the range [48,2047] encode a 2000 levels throttle command.
- Telemetry request: When this bit is high, telemetry is hight, the ESC is sends a telemetry information packet from the to the FC. Including information such as: Motor Electrical RPM, ESC Temperature, Supply Voltage, Current (Available only in certain ESCs). This telemetry message is sent via another pin using Universal Asynchronous Receiver/Transmitter protocol (UART) at 115200 baudrate.
- Cyclic Redundancy Check (CRC): Used to check for data corruption during transmission.

Bidirectional Dshot: This protocol uses exactly the same signal from the ESC to the FC. The difference is the medium of transfer for the Telemetry signal. In this case, the telemetry packet is sent to the FC through the same throttle pin.

Proshot: The data side of this protocol works the same way as Dshot. The 16 bit digital signal is set as a 4 pulse train where each pulse can encode 4 pulse widths (as opposed to only 2 in Dshot).

UAVCAN: As its name suggests, this a full level software platform based on the Controller Area Network (CAN) bus. It supports two-way communication between multiple agents over a twisted pair wire. The signals sent are merely digital (Only high and low voltages at same duration). The protocol packet convention is illustrated in Figure 2.6. Where the elements are explained in [7] as:

- SOF (1 bit): Dominant Start of Frame bit. Used for synchronization.
- Identifier (11-bits): Establishes message priority.
- RTR (1 bit): Remote Transmission Request. Asks next node for transmission.
- IDE (1 bit): Identifies if standard CAN is used or not.
- r0 (1 bit): Reserved.
- DLC (4 bits): Data length. Number of bytes transmitted.
- Data (1-64 bits): Actual data transmitted.
- CRC (16 bits): Cyclic redundancy check.
- ACK (1 bit): Indicates error free reception.

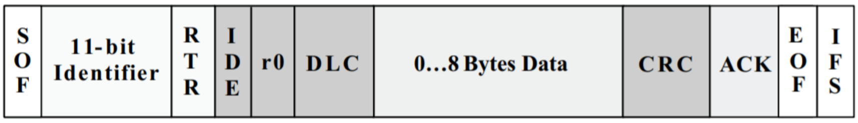

Figure 2.6: CAN bus protocol [7]

- EOF (7 bits): Indicates end of packet.
- IFS (7 bits): Time required to buffer data.

Hence, communication in this protocol is very reliable on the expense of having to send many extra bits for agent coordination and error checking. The maximum bitrate allowed in this protocol is $1Mbit/s$. However, its data transfer rate is decreased by the number of agents connected together and the amount of data each sends. If only one ESC was connected with the FC, the absolute maximum theoretical data rate would be 4.3kHz. Another problem that could arise when using this protocol is significant delays between each rotor command especially between the first motor and the last motor to receive commands. This is because each agent needs to queue when receiving and sending messages as the bus is shared.

2.3 Related Work on ESCs characterization

There have been some studies regarding modeling and characterization BLDC motors driving hardware, given the popularity of their use in UAVs in the last decade. There have been studies in both efficiency and estimation modeling for their dynamic behavior.

2.3.1 Efficiency

Regarding efficiency estimation, several power loss models have been developed based on non-ideal electronic components in the ESCs. Indeed, [8, 9] propose linear and non-linear models for ESC efficiency. There, it is shown that the efficiency changes depending on voltage powering the ESC and current provided to the motor. Furthermore, [10, 11] define complete models of power loss calculation for ESCs driving BLDC motors and [12] models MOSFET power losses. These factors were accounted for in a more generalized model described in [13] and summarized in Equation 2.1.

$$P_{loss} = R_{eq} I_o^2 + (\alpha I_o + \beta) V_{bus} + C f_{eq} V_{bus}^2 \, . \tag{2.1}$$

In this equation, R_{eq} represents the MOSFET on resistance usually given in datasheets, I_o the output current, $V_b us$ the battery voltage, α and β are model values and Cf_{eq} is the equivalent capacitance frequency product for overall circuit.

2.3.2 Modeling for Control

Another stream of research is dedicated to determine the input-output characteristics of ESC-BLDC motor behavior.

Direct Throttle to Thrust mapping is subject of investigation by many sources. A linear first order differential relationship about operating points is proposed by [14], with only two determined parameters: gain and time constant. This model was further improved by [15] by introducing a dead-time parameter to account for communication delays and buffer timing which makes it non-linear. Supply Voltage is show as another parameter that affects ESC-Throttle mapping in [16] where they define a linear MIMO representation with voltage and throttle as inputs; and current and thrust as output, including non-linear elements.

Other studies have instead focused on the Throttle - rotor speed correspondence. In this category, [17] encountered non-linear steady state mapping. Furthermore, one of the first models that incorporated voltage is given by [18] where the steady state value is defined rotor speed is defined as proportional to the voltage and a first order polynomial of the throttle value, and the dynamics still as a first order differential function, these relationships are detailed in Equations 2.2.

$$\frac{\omega}{V} = at + b \quad and \quad \frac{\omega/V}{t} = \frac{k}{\tau s + 1} \,. \tag{2.2}$$

Where a and b are linear fit parameters based on linear fit of steady state data, k and τ are gain and time constant. ω represents rotor speed, V battery voltage and t throttle signal.

Another stream of investigation in this area focused on frequency methods to identify the responses to throttle commands. Chirp sinusoid input throttle signals are used in [19] and the rotor speed output is analyzed. They define a first order differential relation for the ESC output voltage and the utilize a sophisticated motor model to transfer as a transfer function between effective voltage on the motor and rotor speed. Their model even includes cogging modeling, specially important at low speeds. Their complete model is third order differential. Besides, [20] uses steady state response and frequency response using staircase and sinusoidal chirp input throttle signals, but analyses the thrust and torque generated. The model is semi-empirical and includes non-linearities such as torque friction, drag and rotor inertia. However, it assumes a PI loop in the ESC to purpose a model, which is not always the case.
The last stream of investigation in this domain, was merely as data analysis. This includes [21] who analyzed thrust, rotor speed and power outputs, which where presented graphically. Additionally [22] also shows graphical representations of efficiency, power, current, voltage, thrust and torque for different thrust inputs.

Chapter 3

Experimental Setup

Chapter 4

ESC charaterization

Chapter 5

Conclusions and Recommendations

Chapter 6

Einige wichtige Hinweise zum Arbeiten mit LaTeX

Nachfolgend wird die Codierung einiger oft verwendeten Elemente kurz beschrieben. Das Einbinden von Bildern ist in LaTeX nicht ganz unproblematisch und hängt auch stark vom verwendeten Compiler ab. Typisches Format für Bilder in LaTeX ist EPS[1] oder PDF[2].

6.1 Gliederungen

Ein Text kann mit den Befehlen `\chapter{.}`, `\section{.}`, `\subsection{.}` und `\subsubsection{.}` gegliedert werden.

6.2 Referenzen und Verweise

Literaturreferenzen werden mit dem Befehl `\citep{.}` und `\citet{.}` erzeugt. Beispiele: ein Buch [23], ein Buch und ein Journal Paper [23, 24], ein Konferenz Paper mit Erwähnung des Autors: Pratt and Williamson [25].
Zur Erzeugung von Fussnoten wird der Befehl `\footnote{.}` verwendet. Auch hier ein Beispiel[3].
Querverweise im Text werden mit `\label{.}` verankert und mit `\cref{.}` erzeugt. Beispiel einer Referenz auf das zweite Kapitel: chapter 6.

6.3 Aufzählungen

Folgendes Beispiel einer Aufzählung ohne Numerierung,

- Punkt 1
- Punkt 2

wurde erzeugt mit:

```
\begin{itemize}
  \item Punkt 1
  \item Punkt 2
\end{itemize}
```

[1] Encapsulated Postscript
[2] Portable Document Format
[3] Bla bla.

Folgendes Beispiel einer Aufzählung mit Numerierung,

1. Punkt 1
2. Punkt 2

wurde erzeugt mit:

```
\begin{enumerate}
  \item Punkt 1
  \item Punkt 2
\end{enumerate}
```

Folgendes Beispiel einer Auflistung,

P1 Punkt 1

P2 Punkt 2

wurde erzeugt mit:

```
\begin{description}
  \item[P1] Punkt 1
  \item[P2] Punkt 2
\end{description}
```

6.4 Erstellen einer Tabelle

Ein Beispiel einer Tabelle:

Table 6.1: Daten der Fahrzyklen ECE, EUDC, NEFZ.

Kennzahl	Einheit	ECE	EUDC	NEFZ
Dauer	s	780	400	1180
Distanz	km	4.052	6.955	11.007
Durchschnittsgeschwindigkeit	km/h	18.7	62.6	33.6
Leerlaufanteil	%	36	10	27

Die Tabelle wurde erzeugt mit:

```
\begin{table}[h]
\begin{center}
 \caption{Daten der Fahrzyklen ECE, EUDC, NEFZ.}\vspace{1ex}
 \label{tab:tabnefz}
 \begin{tabular}{ll|ccc}
 \hline
 Kennzahl & Einheit & ECE & EUDC & NEFZ \\ \hline \hline
 Dauer & s & 780 & 400 & 1180 \\
 Distanz & km & 4.052 & 6.955 & 11.007 \\
 Durchschnittsgeschwindigkeit & km/h & 18.7 &  62.6 & 33.6 \\
 Leerlaufanteil & \% & 36 & 10 & 27 \\
 \hline
 \end{tabular}
\end{center}
\end{table}
```

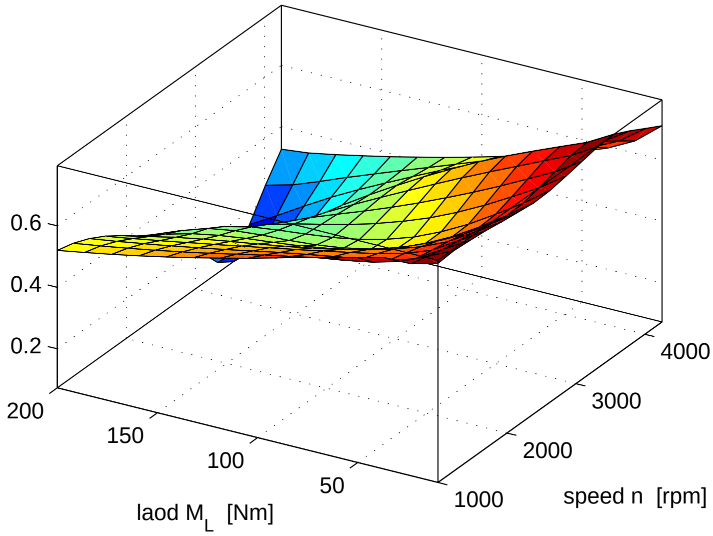

Figure 6.1: Ein Bild

6.5 Einbinden einer Grafik

Das Einbinden von Graphiken kann wie folgt bewerkstelligt werden:

```
\begin{figure}
   \centering
   \includegraphics[width=0.75\textwidth]{images/k_surf.pdf}
   \caption{Ein Bild.}
   \label{fig:k_surf}
\end{figure}
```

oder bei zwei Bildern nebeneinander mit:

```
\begin{figure}
  \begin{minipage}[t]{0.48\textwidth}
    \includegraphics[width = \textwidth]{images/cycle_we.pdf}
  \end{minipage}
  \hfill
  \begin{minipage}[t]{0.48\textwidth}
    \includegraphics[width = \textwidth]{images/cycle_ml.pdf}
  \end{minipage}
  \caption{Zwei Bilder nebeneinander.}
  \label{pics:cycle}
\end{figure}
```

6.6 Mathematische Formeln

Einfache mathematische Formeln werden mit der equation-Umgebung erzeugt:

$$p_{me0f}(T_e, \omega_e) \;=\; k_1(T_e) \cdot (k_2 + k_3 S^2 \omega_e^2) \cdot \Pi_{\max} \cdot \sqrt{\frac{k_4}{B}}\,. \tag{6.1}$$

Der Code dazu lautet:

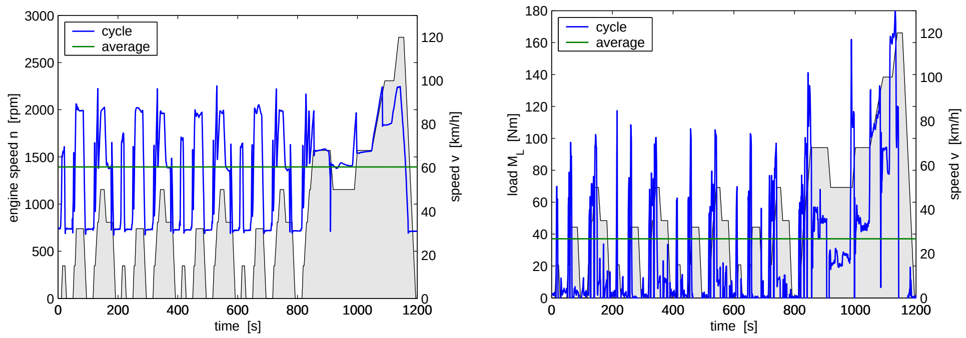

Figure 6.2: Zwei Bilder nebeneinander

```
\begin{equation}
 p_{me0f}(T_e,\omega_e) \ = \ k_1(T_e) \cdot (k_2+k_3 S^2
 \omega_e^2) \cdot \Pi_{max} \cdot \sqrt{\frac{k_4}{B}} \, .
\end{equation}
```

Mathematische Ausdrücke im Text werden mit $formel$ erzeugt (z.B.: $a^2+b^2=c^2$). Vektoren und Matrizen werden mit den Befehlen `\vec{.}` und `\mat{.}` erzeugt (z.B. $\boldsymbol{v}$, $\boldsymbol{M}$).

6.7 Weitere nützliche Befehle

Hervorhebungen im Text sehen so aus: *hervorgehoben*. Erzeugt werden sie mit dem `\epmh{.}` Befehl.
Einheiten werden mit den Befehlen `\unit[1]{m}` (z.B. 1 m) und `\unitfrac[1]{m}{s}` (z.B. 1 m/s) gesetzt.

Bibliography

[1] K. Bodie, Z. Taylor, M. Kamel, and R. Siegwart, "Towards Efficient Full Pose Omnidirectionality with Overactuated MAVs," in *Proceedings of the 2018 International Symposium on Experimental Robotics*, J. Xiao, T. Kröger, and O. Khatib, Eds. Cham: Springer International Publishing, 2020, pp. 85–95.

[2] M. Allenspach, K. Bodie, M. Brunner, L. Rinsoz, Z. Taylor, M. Kamel, R. Siegwart, and J. Nieto, "Design and optimal control of a tiltrotor micro aerial vehicle for efficient omnidirectional flight," 2020.

[3] J. Zhao and Y. Yu, "Brushless DC Motor Fundamentals," Monolithic Power Systems, Tech. Rep., 2011.

[4] K. Mogensen, "Motor-control considerations for electronic speed control in drones," *Analog Applications Journal*, pp. 1–7, 2016.

[5] Backyard Robotics, "On ESC Protocols Part II," 2018.

[6] Speedgoat, "Dshot usage notes," 2020.

[7] S. Corrigan, "Introduction to the Controller Area Network (CAN)," Texas Instruments, Tech. Rep., 2016.

[8] A. Gong and D. Verstraete, "Experimental testing of electronic speed controllers for UAVs," in *53rd AIAA/SAE/ASEE Joint Propulsion Conference, 2017*, 2017.

[9] A. Gong, R. Macneill, and D. Verstraete, "Performance Testing and Modeling of a Brushless DC Motor, Electronic Speed Controller and Propeller for a Small UAV Application," 2018.

[10] P. Millett, "Calculating Motor Driver Power Dissipation," Texas Instruments, Dallas, Texas, Tech. Rep., 2012.

[11] A. Keskar, N. and Batello, M. and Guerra, A. and Gorgerino, "Application Note AN-1048: Power Loss Estimation in BLDC Motor Drives Using iCalc," International Rectifier, Tech. Rep.

[12] M. Graovac, Dušan and Pürschel, "MOSFET Power losses Calculation Using the Data-sheet Parameters," Infineon, Neubiberg, Germany, Tech. Rep., 2006.

[13] Tritium, "WaveSculptor 22 Motor Drive User's Manual," Tritium, Tech. Rep., 2013.

[14] M. Yoon, "Experimental Identification of Thrust Dynamics for a Multi-Rotor Helicopter," *International Journal of Engineering Research & Technology (IJERT)*, vol. 4, no. 11, pp. 206–209, 2015.

[15] R. T. Torres and F. Sergii, "Brushless Direct Current Propulsion System Identification," in *Integrated Computer Technologies in Mechanical Engineering*, M. Nechyporuk, V. Pavlikov, and D. Kritskiy, Eds. Cham: Springer International Publishing, 2020, pp. 105–113.

[16] G. Szafranski, R. Czyba, and M. BŁachuta, "Modeling and identification of electric propulsion system for multirotor unmanned aerial vehicle design," in *2014 International Conference on Unmanned Aircraft Systems (ICUAS)*, 2014, pp. 470–476.

[17] J. A. Prakosa, D. V. Samokhvalov, G. R. V. Ponce, and F. Sh. Al-Mahturi, "Speed Control of Brushless DC Motor for Quad Copter Drone Ground Test," in *2019 IEEE Conference of Russian Young Researchers in Electrical and Electronic Engineering (EIConRus)*, 2019, pp. 644–648.

[18] A. Moutinho, E. Mateos, and F. Cunha, "The Tilt-Quadrotor: Concept, Modeling and Identification," in *2015 IEEE International Conference on Autonomous Robot Systems and Competitions*, 2015, pp. 156–161.

[19] C. Xiang, X. Wang, Y. Ma, and B. Xu, "Practical Modeling and Comprehensive System Identification of a BLDC Motor," *Hidawi Publishing Coorporation*, vol. 2015, pp. 1024–123X, 2015.

[20] L. Wu, Y. Ke, and B. Chen, "Systematic Modeling of Rotor-Driving Dynamics for Small Unmanned Aerial Vehicles," *Unmanned Systems*, vol. 6, no. 2, pp. 81–93, 2018.

[21] D. Kotarski, M. Krznar, P. Piljek, and N. Simunic, "Experimental Identification and Characterization of Multirotor {UAV} Propulsion," *Journal of Physics: Conference Series*, vol. 870, p. 12003, jul 2017.

[22] M. Sulewski, L. Ambroziak, M. Kondratiuk, and A. Stulgis, "Identification of electric propulsion system for unmanned aerial vehicles," *AIP Conference Proceedings*, vol. 2029, no. 1, p. 20072, 2018.

[23] M. Raibert, *Legged Robots That Balance.* Cambridge, MA: MIT Press, 1986.

[24] M. Vukobratović and B. Borovac, "Zero-moment point — thirty five years of its life," *International Journal of Humanoid Robotics*, vol. 1, no. 01, pp. 157–173, 2004.

[25] G. A. Pratt and M. M. Williamson, "Series elastic actuators," in *IEEE/RSJ International Conference on Intelligent Robots and Systems (IROS)*, 1995, pp. 3137–3181.

Appendix A

Irgendwas

Bla bla . . .

Appendix B

Datasheets

EC-max 30 ∅30 mm, brushless, 60 Watt

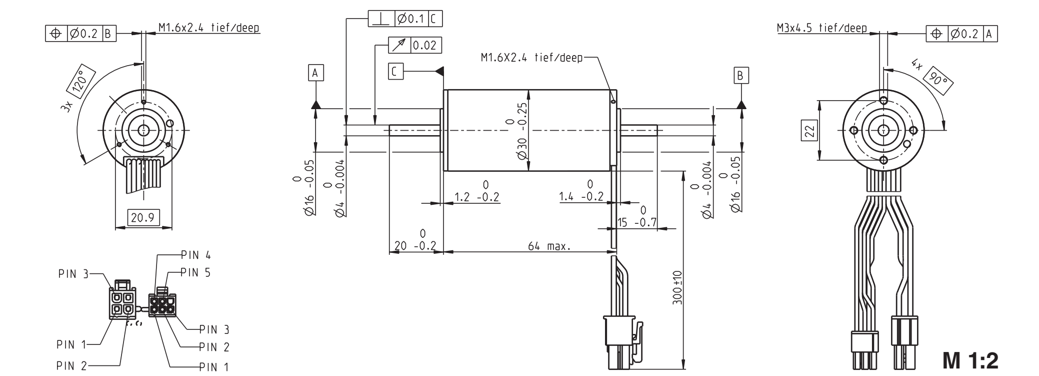

maxon EC-max

Stock program
Standard program
Special program (on request)

Part Numbers

Motor Data		272762	272763	272764	272765
Values at nominal voltage					
1 Nominal voltage	V	12	24	36	48
2 No load speed	rpm	7980	9340	9490	9350
3 No load current	mA	302	191	130	95.4
4 Nominal speed	rpm	6590	8040	8270	8130
5 Nominal torque (max. continuous torque)	mNm	63.6	60.7	63.7	64.1
6 Nominal current (max. continuous current)	A	4.72	2.66	1.88	1.4
7 Stall torque	mNm	381	458	522	519
8 Starting current	A	26.8	18.8	14.5	10.7
9 Max. efficiency	%	80	81	82	82
Characteristics					
10 Terminal resistance phase to phase	Ω	0.447	1.27	2.48	4.49
11 Terminal inductance phase to phase	mH	0.049	0.143	0.312	0.573
12 Torque constant	mNm/A	14.2	24.3	35.9	48.6
13 Speed constant	rpm/V	672	393	266	197
14 Speed/torque gradient	rpm/mNm	21.2	20.6	18.4	18.2
15 Mechanical time constant	ms	4.86	4.73	4.21	4.17
16 Rotor inertia	gcm²	21.9	21.9	21.9	21.9

Specifications

Thermal data

17	Thermal resistance housing-ambient	7.4 K/W
18	Thermal resistance winding-housing	0.5 K/W
19	Thermal time constant winding	2.76 s
20	Thermal time constant motor	1000 s
21	Ambient temperature	-40…+100°C
22	Max. permissible winding temperature	+155°C

Mechanical data (preloaded ball bearings)

23	Max. permissible speed	15000 rpm
24	Axial play at axial load < 6.0 N	0 mm
	> 6.0 N	0.14 mm
25	Radial play	preloaded
26	Max. axial load (dynamic)	5 N
27	Max. force for press fits (static)	98 N
	(static, shaft supported)	1300 N
28	Max. radial loading, 5 mm from flange	25 N

Other specifications

29	Number of pole pairs	1
30	Number of phases	3
31	Weight of motor	305 g

Values listed in the table are nominal.

Connection motor (Cable AWG 20)

red	Motor winding 1	Pin 1
black	Motor winding 2	Pin 2
white	Motor winding 3	Pin 3
	N.C.	Pin 4
Connector	**Part number**	
Molex	39-01-2040	

Connection Sensors (Cable AWG 26)

yellow	Hall sensor 1	Pin 1
brown	Hall sensor 2	Pin 2
grey	Hall sensor 3	Pin 3
blue	GND	Pin 4
green	V_{Hall} 3…24 VDC	Pin 5
	N.C.	Pin 6
Connector	**Part number**	
Molex	430-25-0600	

Wiring diagram for Hall sensors see p. 35

Operating Range

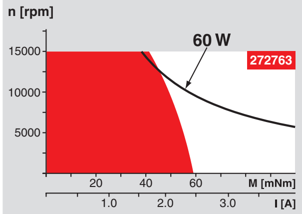

Comments

Continuous operation
In observation of above listed thermal resistance (lines 17 and 18) the maximum permissible winding temperature will be reached during continuous operation at 25°C ambient.
= Thermal limit.

Short term operation
The motor may be briefly overloaded (recurring).

Assigned power rating

maxon Modular System Overview on page 20 - 25

Planetary Gearhead
∅32 mm
8.0 Nm
Page 266

Koaxdrive
∅32 mm
1.0 - 4.5 Nm
Page 268

Planetary Gearhead
∅42 mm
3 - 15 Nm
Page 271

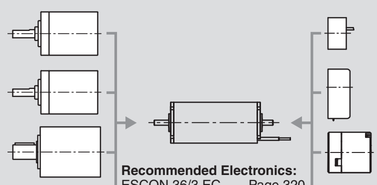

Encoder MR
500/1000 CPT,
3 channels
Page 302

Encoder HEDL 5540
500 CPT,
3 channels
Page 308

Brake AB 20
24 VDC
0.1 Nm
Page 346

Recommended Electronics:

ESCON 36/3 EC	Page 320
ESCON 50/5, Module 50/5	321
ESCON 70/10	321
DECS 50/5	324
DEC Module 24/2	325
DEC Module 50/5	325
EPOS2 24/5, 50/5	331
EPOS2 P 24/5	334
EPOS3 70/10 EtherCAT	337
Notes	**24**

RE 40 ∅40 mm, Precious Metal Brushes, 25 Watt

NEW

maxon DC motor

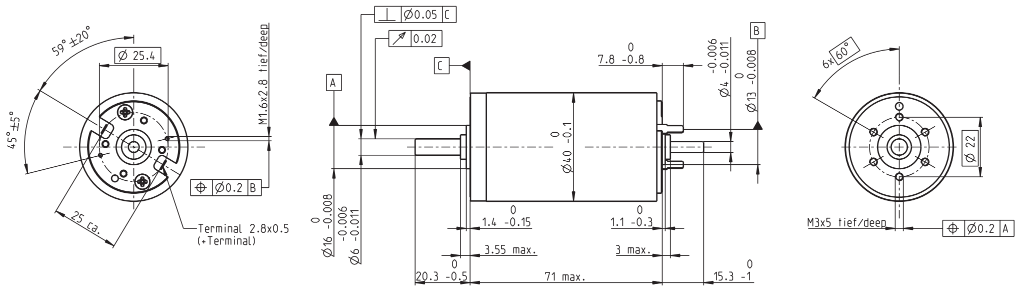

M 1:2

Stock program
Standard program
Special program (on request)

		Part Numbers						
		448588	448589	448590	448591	448592		
Motor Data								
Values at nominal voltage								
1 Nominal voltage	V	9	18	24	42	48		
2 No load speed	rpm	2850	2850	2780	2920	2690		
3 No load current	mA	49.7	24.8	18.1	11	8.62		
4 Nominal speed	rpm	2610	2600	2480	2640	2410		
5 Nominal torque (max. continuous torque)	mNm	87.8	87.8	88.2	87.6	87.6		
6 Nominal current (max. continuous current)	A	2.96	1.48	1.09	0.65	0.524		
7 Stall torque	mNm	873	956	794	895	818		
8 Starting current	A	29	15.9	9.66	6.53	4.81		
9 Max. efficiency	%	92	92	92	92	92		
Characteristics								
10 Terminal resistance	Ω	0.311	1.14	2.49	6.43	9.97		
11 Terminal inductance	mH	0.0824	0.33	0.613	1.7	2.62		
12 Torque constant	mNm/A	30.2	60.3	82.2	137	170		
13 Speed constant	rpm/V	317	158	116	69.7	56.2		
14 Speed / torque gradient	rpm/mNm	3.27	2.98	3.51	3.27	3.3		
15 Mechanical time constant	ms	4.85	4.29	4.36	4.14	4.13		
16 Rotor inertia	gcm²	142	137	119	121	120		

Specifications

Thermal data

17 Thermal resistance housing-ambient	4.65 K/W
18 Thermal resistance winding-housing	1.93 K/W
19 Thermal time constant winding	41.5 s
20 Thermal time constant motor	809 s
21 Ambient temperature	-20…+85°C
22 Max. permissible winding temperature	+100°C

Mechanical data (ball bearings)

23 Max. permissible speed	3330 rpm
24 Axial play	0.05 - 0.15 mm
25 Radial play	0.025 mm
26 Max. axial load (dynamic)	5.6 N
27 Max. force for press fits (static)	110 N
(static, shaft supported)	1200 N
28 Max. radial loading, 5 mm from flange	28 N

Other specifications

29 Number of pole pairs	1
30 Number of commutator segments	13
31 Weight of motor	480 g

Values listed in the table are nominal.
Explanation of the figures on page 71.

Option
Preloaded ball bearings

Operating Range

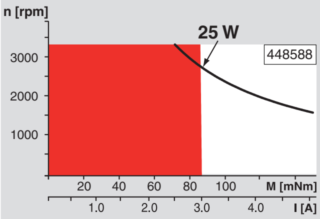

Comments

Continuous operation
In observation of above listed thermal resistance (lines 17 and 18) the maximum permissible winding temperature will be reached during continuous operation at 25°C ambient.
= Thermal limit.

Short term operation
The motor may be briefly overloaded (recurring).

Assigned power rating

maxon Modular System

Overview on page 20 - 25

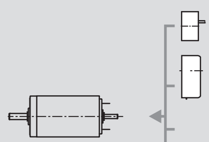

Encoder MR
256 - 1024 CPT,
3 channels
Page 303

Encoder HED_ 5540
500 CPT,
3 channels
Page 305/307

Recommended Electronics:

ESCON 36/2 DC	Page 320
ESCON 50/5	321
ESCON Module 50/5	321
EPOS2 24/2	330
EPOS2 Module 36/2	330
EPOS2 24/5	331
EPOS2 50/5	331
EPOS2 P 24/5	334
EPOS3 70/10 EtherCAT	337
Notes	**22**